

# 3D-Simulation of a Bayard Alpert ionisation gauge using Simion program

Ricardo Silva, Nenad Bundaleski\*, Ana Fonseca, Orlando Teodoro

*CeFiTec, Departamento de Física, Faculdade de Ciências e Tecnologia, Universidade*

*Nova de Lisboa, Portugal*

\*Corresponding author: Tel: +351 212 948 300; fax: +351 212 954 461

e-mail address: [n.bundaleski@fct.unl.pt](mailto:n.bundaleski@fct.unl.pt)

Numerical simulation of an ionisation gauge using SIMION 8.1 software is presented. The gauge sensitivity, being the most important parameter of an ionisation gauge, has been derived using two different approaches. In the first, the estimative one, SIMION is used to determine mean length of electron trajectories, and the ion collection efficiency. From these values, and the known ionisation cross sections and the gas temperature, the sensitivity can be readily calculated. In the second and more detailed approach, a Monte Carlo method was implemented in the Lua program to simulate the electron impact ionisation of the gas. The Lua code is incorporated in the Simion trajectory simulations, in which the ionisation event is modelled as a transformation of a primary electron particle into an ion. This approach evaluates the contribution of each trajectory to the gas ionisation. Besides, it considers energy dependence of the ionisation probability, and the contribution of the electrons backscattered from the grid to the sensitivity. The simulation approaches were tested on the example a Bayard Alpert gauge that was recently modelled by the CERN group. Very good quantitative agreement with the CERN simulations was obtained using both approaches. Monte Carlo simulations reveal

that the relative contribution of electrons backscattered from the molybdenum grid to the sensitivity is about 14 %.

Keywords: Vacuum, Ionisation gauges, Simulation, Sensitivity

## 1. Introduction

Ionisation gauge (IG) is the only vacuum gauge type for high and ultrahigh vacuum ranges, which are of extreme significance for both science and industry. However, these devices are lacking of robustness, long-term and transport stabilities. In the case of the particularly popular Bayard Alpert ionisation gauge (BA), the sensitivity tends to decrease with time. Besides, gauge to gauge variations defined as one standard deviation are typically within  $\pm 15-30$  %, while successive calibrations may have difference of about 3-6 %, depending on the type of the filament [1, 2]. The first step in solving these problems is in understanding all details of IG operation. In that respect, reliable simulations do not give only the insight into the sources of instabilities [3-5], but also represent powerful tools for the design of more reliable devices [6, 7].

Modelling the operation of ionisation gauges is closely related to the simulation of the corresponding electron and ion trajectories. In many cases, the calculations were simplified by performing 2D calculations [5, 6] of the field distributions or eventually 3D calculations of systems with cylindrical symmetry [4].

True 3D simulations of the charged particle optics in IGs were firstly performed by Kauert and co-authors using a home-made program IONTRA3d [8]. In this approach, the field distribution inside the ionisation gauges has been performed by solving the Laplace equation by the finite difference method. The gas ionisation was modelled using the Monte Carlo method in the pressure range close or above the upper

limit of IGs ( $10^{-3} - 10$  mbar) in order to increase the number of ionisation events. Recently, an IG simulation tool based on the OPERA software package was recently developed in CERN. The simulations of the home-made BA and Helmer gauges reasonably agree with the experiments [9]. To our knowledge, these simulations perform the first detailed treatment of the space charge effects in IGs.

The aim of this work is to develop our own IG simulation tools based on the well-known and widely spread software for the charged particle optics simulation, Simion ver. 8.1. Two approaches for the evaluation of the ionisation gauge sensitivity are proposed. The first one is very simple to apply for any Simion user, and should serve as a first estimation of the IG sensitivity. The second one is based on the ability of Simion to couple calculation of charged particles trajectories with a script code (written in Lua programming language) developed by the user. In this case, the code represents a Monte Carlo simulation of electron impact ionisation of the gas molecules. In addition, it opens a possibility to add additional effects. At this point, the code is also used to model the electron backscattering from the grid, which increases the electron trajectory length and consequently the IG sensitivity. Both approaches were used to simulate the home-made BA gauge from CERN. The simulation results are compared with those reported in [9].

## 2. Description of the models

In every hot-filament ionisation gauge, electrons are emitted from the cathode by the thermionic emission. After their acceleration, the electrons collide with gas molecules and eventually ionise them. The ions are then attracted by the collector electrode, and therefore detected as a positive ion current  $I_{ion}$ . The intensity of the ion current can be expressed as  $I_{ion} = I_e \cdot P_{ion} \cdot P_{coll}$ , where  $I_e$  is the electron emission current,

$P_{ion}$  is the ionisation probability and  $P_{coll}$  is the probability that the generated ion will reach the collector electrode (also known as collection efficiency). The ionisation probability in the case of a monoenergetic electron equals

$$P_{ion}=1 - e^{-\frac{L}{\lambda}}, \quad (1)$$

where  $L$  is the electron path length and  $\lambda$  is the mean path between the two ionisation events [4]. The mean free path can be expressed as  $\lambda=1/(n\cdot\sigma)$ , where  $\sigma$  is the electron impact ionisation cross-section, and  $n$  is the gas concentration in the gauge. Since  $L\ll\lambda$  in the pressure range of interest, eq. (1) can be linearized. After expressing  $n$  by the gas pressure  $p$  and the gas temperature  $T$ , the ion current can be formulated as

$$I_{ion}=I_e\cdot p\cdot\frac{L\cdot\sigma}{kT}\cdot P_{coll}=I_e\cdot p\cdot S, \quad (2)$$

where  $k$  is the Boltzmann constant and  $S$  is the sensitivity of the ionisation gauge. Sensitivity is the most important parameter of any IG, defining the relation between the pressure, electron emission current and the ion current. It should be noted that the eq. (2) is valid only when  $L \ll \lambda$ , so that the ionisation probability can be linearized. At higher pressures the linear dependence between  $I_{ion}$  and  $p$  should not hold anymore.

## 2.1 Estimative approach

It can be seen from eq. (2) that the sensitivity of an IG can be easily calculated from the known electron path length  $L$  and the collection efficiency  $P_{coll}$ . Apparently any software for the charged particle optics can serve for determining these two values. Our simulations were performed by the well-known program Simion ver. 8.1. The electron path length strongly depends on the initial conditions (i.e. the point of the filament from which an electron is emitted and from its initial direction), yielding in a rather wide distribution of  $L$ . Here we use its mean value  $\langle L \rangle$  to calculate the sensitivity. For each electron trajectory of length  $L$ , one ion is created at the point

determined by  $w = RND \cdot L$ , where  $RND$  is uniformly distributed random number in the range  $[0, 1]$ . The creation point is situated along the electron trajectory at the distance  $w$  from the beginning of the trajectory. The initial velocity of ions is randomly chosen, and follows the Maxwell distribution. The collection efficiency is calculated as a fraction of ions that reach the collector electrode. The maximum energy that electrons can have along their trajectory is determined by the voltage difference between the grid and the filament. The value of the ionisation cross section used in the expression for  $S$  is calculated for the pumped gas and the electron energy somewhat lower than their maximum energy.

This simplified and readily applicable approach in evaluating the sensitivity of an IG has a few potential drawbacks. First of all, it is an open question whether the mean electron path length is a good representative of all electron trajectories. Secondly, the electrons are changing their energy, and consequently the ionisation cross section, along the trajectory. Therefore, using a single and rather arbitrary value for  $\sigma$  will likely introduce a systematic error.

The question of the gas temperature should be also considered, particularly when comparing the calculated sensitivity (using any approach) with the experimental values. Clearly, gas temperature inside the ionisation region of an IG is elevated due to the filament operation, which also heats the grid and the nearby chamber walls. IGs actually measures gas concentration inside the ionisation volume. If the whole system is isothermal the gas should be uniformly distributed in the vacuum vessel. Higher temperature would mean higher pressure for the same concentration and consequently, the sensitivity is reduced (see eq. 2). If the gas in the ionisation volume is warmer than in the rest of the vessel, which is much more likely, the gas flow from the ionisation volume will take place due to the thermal transpiration. In equilibrium, the ratio of

pressures in the ionisation volume and in the rest of the vacuum vessel will equal the square root of the corresponding temperature ratio. The estimated gas temperature difference between the chamber and the ionisation volume may span from 70 to 220 K depending on the IG type [10]. Finally, higher temperatures and the electrons inside the IG volume contribute to outgassing and electron stimulated desorption, which additionally increase the local gas concentration. All these issues will affect the experimentally obtained IG sensitivity. On the other hand, eq. (2) relates the pressure and gas temperature inside an IG with its sensitivity, and should therefore always hold as long as  $L \ll \lambda$ .

## 2.2 Monte Carlo simulation

The main idea of this approach has some similarities with that of Kauert and co-workers [8]. The electron trajectory in an IG is calculated by Simion. At the same time, the electron impact ionisation events are modelled by Monte Carlo method. From the known  $p$  and  $\sigma$  (which is electron energy dependent) one can easily calculate the ionisation probability along the trajectory segment of length  $dL$ ,  $P_{ion}(dL)$ . If so, uniformly distributed random number  $RND$  can be compared with  $P_{ion}$ . If the ionisation event did not take place, the Simion proceeds with the calculation of the electron trajectory. Otherwise, the electron is transformed into an ion. Simion then continues to follow the ion trajectory, which may end up on a collector electrode (the ion contributes to  $I_{ion}$ ) or at the chamber wall. At the end of the simulation, the sensitivity is obtained as the number of collected ions divided by the total electron number.

Although simple to implement, such general algorithm is extremely inefficient since vast majority of electrons do not produce any ions. Indeed, assuming a typical value of sensitivity  $S = 10 \text{ mbar}^{-1}$  and  $p = 10^{-5} \text{ mbar}$ , one ion will be created per 10000

electrons! This problem has been tackled in [8] by performing simulation only at pressures in the range  $10^{-3}$  - 10 mbar. Apart from the inappropriate pressure range, the main problem with this ‘solution’ is that the condition  $L \ll \lambda$  does not hold anymore: there is a finite probability that one electron may ionise more than one molecule. If so, the electron energy loss due to the ionisation should be also considered, as well as the emission of an extra electron. However, these complex processes were ignored in [8].

In this work, we increase the efficiency of the simulation by addressing to each trajectory a bunch of  $N$  electrons, which roughly increases the ionisation probability  $N$  times. Since  $N$  electrons can theoretically make more than a single ion, transformation of the whole bunch of electrons into an ion can in some cases reduce the sensitivity factor. Consequently, the number  $N$  of electrons represented by a single trajectory has to be chosen carefully, in order to prevent significant reduction of the sensitivity factors.

### 2.2.1. Calculation of the number of electrons in the bunch

Assuming that ionisation events are mutually independent, the probability that the bunch of  $N$  electrons will create  $k$  ions along the trajectory  $r$  can be expressed as the binomial distribution  $P(N,k) = \binom{N}{k} p_1(r)^k \cdot (1 - p_1(r))^{N-k}$ , where  $p_1$  is the probability that a single electron will create an ion along the trajectory  $r$ . This probability can be calculated as

$$p_1 = 1 - \exp(-n \int \sigma dr), \quad (3)$$

where the integration is performed along the trajectory  $r$ . This expression is a generalization of the eq. (1), encompassing the case of an electron which is changing the energy along the trajectory. If  $N$  is too small, gas ionisation will still be extremely rare event; in the other extreme, the probability of creating more than one ion by the bunch will not be negligible. The optimal number of electrons was calculated so that the sum

of probabilities to create 0 or 1 ion is greater than some predefined value  $\varepsilon$ , nearly equal to 1:

$$P(N_i, 0) + P(N_i, 1) = (1 - p_1(r_i))^{N_i} + N_i \cdot p_1(r_i) \cdot (1 - p_1(r_i))^{N_i-1} > \varepsilon, \quad (4)$$

For each trajectory  $r_i$ ,  $N_i$  is calculated as the maximum integer satisfying the inequality (4) using the bisection method. In our calculations the value of  $\varepsilon$  was 0.99.

### 2.2.2. Fast calculation of the ionisation cross sections

The ionisation cross sections of  $N_2$  and  $H_2$  are originally calculated using the Binary-Encounter-Bethe (BEB) model [11]. Since the analytical calculation from this model is time consuming (summation has to be carried over each molecular orbital), this data were fitted to the approximate analytical formula

$$\sigma(E) = \frac{1}{IE} \left[ A \cdot \ln \left( \frac{E}{I} \right) + \sum_{i=1}^N B_i \cdot \left( 1 - \frac{I}{E} \right)^i \right], \quad (5)$$

proposed in [12] for the ionisation cross sections of single atoms. In the eq. (5),  $I$  is the ionisation potential of the molecule in eV, while  $A$  and  $B_i$  are the fitting parameters.

**There is an error in the formula (5) shown in [12] – they omit the power ‘i’.** Although it works very well for energies  $E > 20$  eV, fitting to this formula introduces considerable error for both molecules and atoms close to the ionisation threshold. Therefore, in the energy range from  $I$  to 20 eV the cross sections are linearly interpolated as  $\sigma(E) = \sigma(20 \text{ eV}) \cdot (E - I) / (20 \text{ eV} - I)$ . This approach provides very good agreement with the BEB model in the whole energy range. The fitting parameters used for the  $\sigma$  calculation of  $N_2$  and  $H_2$  are presented in Table 1.

Table 1. Coefficients for the ionisation cross section calculation for N<sub>2</sub> and H<sub>2</sub>.

Molecule	H <sub>2</sub>	N <sub>2</sub>
A (Å <sup>2</sup> eV <sup>2</sup> )	757.5	2099.35
B <sub>1</sub> (Å <sup>2</sup> eV <sup>2</sup> )	-1093.7	7573.1
B <sub>2</sub> (Å <sup>2</sup> eV <sup>2</sup> )	-10489	-184897
B <sub>3</sub> (Å <sup>2</sup> eV <sup>2</sup> )	-66634	1.24366·10 <sup>6</sup>
B <sub>4</sub> (Å <sup>2</sup> eV <sup>2</sup> )	202530	3.9080·10 <sup>6</sup>
B <sub>5</sub> (Å <sup>2</sup> eV <sup>2</sup> )	-311073	6.27301·10 <sup>6</sup>
B <sub>6</sub> (Å <sup>2</sup> eV <sup>2</sup> )	235011	-4.98371·10 <sup>6</sup>
B <sub>7</sub> (Å <sup>2</sup> eV <sup>2</sup> )	68532	1.55924·10 <sup>6</sup>

### 2.2.3 Detailed description of the algorithm

Each trajectory, defined by the initial conditions, is run two times. The first run is used to calculate the number of electrons in the bunch  $N$ . The actual simulation is performed in the second run. For each trajectory segment  $dL$  the probability of the electron impact ionisation is calculated as  $P_{ion}(dL) = dL \cdot \sigma(E) \cdot p/kT$ . Note that this expression is equivalent to the linear approximation introduced when deriving the expression for the sensitivity. The approximation for the trajectory segment is much more applicable than in the expression (1) for the ionisation probability where the total electron trajectory length is considered.

In the next step, the probability of the electron ionisation by the bunch of  $N$  electrons is calculated as  $P_{ion,N}(dL) = N \cdot P_{ion}(dL) \cdot (1 - P_{ion}(dL))^{N-1}$ . In the Monte Carlo simulation, a uniformly distributed random number  $RND$  is compared with  $P_{ion,N}(dL)$ :

- A. If  $RND < P_{ion,N}(dL)$ , the ionisation took place – electron bunch is transformed into a single gas ion. The initial ion velocity is chosen randomly so that it follows Maxwell distribution defined by the gas temperature and mass, which are input parameters. The transformation of the uniform into the normal distribution of random values is performed using the Box-Muller transform. Simion proceeds with the calculation of the ion trajectory.
- B. Otherwise, Simion proceeds with the calculation of the electron trajectory.

At the moment of electron collision with an electrode, we also consider the possibility of electron backscattering using the approach described in the next section.

#### 2.2.4 Modelling of the electron backscattering

In this model we consider only backscattered electrons, which are formally separated from the so-called true secondary electrons by their kinetic energy  $E > 50$  eV [13]. The quantity of backscattered electrons is described by the backscattering yield (*BSY*), defined as the number of backscattered electrons emitted per incident electron. Electron backscattering is also modelled by the Monte Carlo method. After the collision of an electron with the grid, a random number uniformly distributed in the range  $[0, 1]$  is generated and compared with *BSY*. The backscattered electron is created only if the random number is lower than *BSY*. The initial velocity of backscattered electrons is defined randomly in such way to reproduce the corresponding angular and energy distributions. The trajectory of backscattered electrons is then calculated by Simion in the same way as that of the primary electrons. The gas ionisation by backscattered electrons is modelled in the same manner as that performed by primary electrons. The number of electrons in the bunch  $N$  is conserved after the backscattering event.

The geometry of the electron backscattering event is depicted in Fig.1. At the moment of the surface impact, the primary electron has a velocity  $\mathbf{v}_{imp}$ . Its incident angle  $\alpha$  is defined with respect to the surface normal  $\mathbf{n}$ . The velocity of the backscattered electron  $\mathbf{v}_{out}$  is determined by its intensity  $v_{out}$ , polar angle  $\theta$ , defined with respect to the surface normal  $\mathbf{n}$ , and the azimuth angle  $\varphi$ , i.e. the angle between the surface projections of the vectors  $\mathbf{v}_{imp}$  and  $\mathbf{v}_{out}$ .

The backscattering yield (*BSY*) and the angular distribution of backscattered electrons are strongly dependent on the primary electron incident angle  $\alpha$ . However,

apart from the *BSY* vs. the electron primary energy at normal incidence, there is hardly any experimental data available. Therefore, the majority of distributions applied in this model are determined using the program Casino ver. 2.48, representing a Monte Carlo simulation of electron-surface interactions [14]. This program provides energy and polar angle distribution (integrated over azimuth angle) of backscattered electrons.

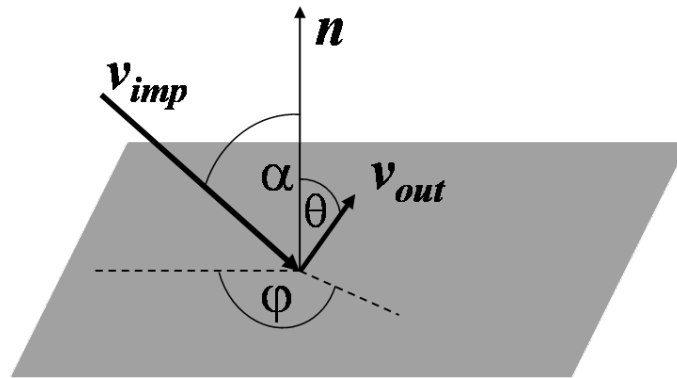


Figure 1. Illustration of the electron backscattering event.

We consider that the grid is made of molybdenum, which is a typical material used for the electrodes in IGs. The electron energy at the moment of interaction with the grid surface is 100 eV. By extrapolating the experimental energy dependence of *BSY* at normal incidence (i.e.  $\alpha = 0^\circ$ ), we estimate that  $BSY(100 \text{ eV}) = 0.15$  [15]. **This is not far from the corresponding simulation result of 0.12.** According to the simulations, *BSY* dependence on the incidence angle can be described as  $BSY(\alpha) = BSY(0^\circ)/(\cos\theta)^{0.7}$ , similar to the equivalent dependence of secondary electrons [13].

Polar angle distributions were determined using the Casino program for 9 equidistant incidence angles ranging from  $0^\circ$  to  $80^\circ$ , and fitted to the 5<sup>th</sup> order polynomial. Azimuth angle distribution was estimated according to the experimental data available for aluminium in the comparable energy range [16]. For incident angle  $\alpha$

in the range  $0^\circ$ - $30^\circ$ ,  $\varphi$  is uniformly distributed in the overall range  $[0^\circ, 360^\circ]$ . When  $\alpha > 30^\circ$ , the electrons are uniformly backscattered with the  $\varphi$  in the range  $90^\circ$ - $270^\circ$ .

### 3. Simulation details

The details of the BA gauge construction and the electrode voltages, provided by CERN, are presented in Figure 2. The gauge is assumed to be mounted inside a cylindrical vacuum chamber with the inner diameter of 63 mm. The dimension of the electrodes are given in Table 2. The IG consists of a grid, ion collector, two filaments and two modulator electrodes used to overcome the X-ray limit of the filament. The filaments are at 50 V, the grid is at 150 V, and the ion collector is grounded. In our simulations we consider only the case with modulators on the grid potential, when the collector current is actually measured. In the trajectory simulations, the inner diameter of the grounded tube in which the gauge is placed was 50 mm.

Table 2. The dimensions of the BA gauge electrodes [9].

Electrode	Dimensions (mm)	Wire diameter
Grid	$\phi$ 35×45	$\phi$ 0.13
Filament	height 30	$\phi$ 0.18
Modulator	length 42	$\phi$ 0.7
Collector	length 42	$\phi$ 0.05
Chamber	$\phi$ 63	–

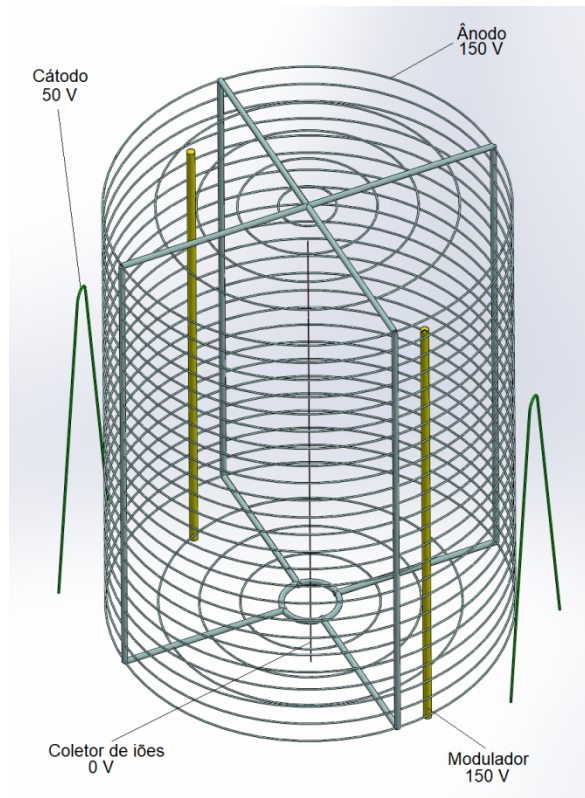


Figure 2. Schematic of the BA ionisation gauge electrodes. The voltages of each electrode are given in the figure. Ricardo, this should be tiff/jpg image with 300 dpi resolution or higher. In addition, translate the text of the picture to English, and increase the font size.

The calculation of electron and ion trajectories in the BA gauge is performed using the program Simion ver. 8.1, in which the geometry was introduced by importing a CAD image. The potential distribution is estimated using the finite difference technique for solving numerically the Laplace equation. The convergence objective for the calculation of the potential distribution was  $5 \cdot 10^{-6}$  of the electrode potential. Further decrease of the convergence objective for 3 orders of magnitude did not affect the trajectory calculations. The cubic grid was employed with the size of 0.05 mm, resulting in huge 3D potential arrays. Further resolution increase would make the execution times of both potential and trajectory calculations too long on an ordinary PC. This resolution

is apparently insufficient for the proper description of the gauge geometry, particularly of the ion collector (see Table 2) which has an irregular shape and width of  $\sim 0.1$  mm in the simulation. However, knowing that the electrons cannot approach close to the ion collector and the ions are thermal, the change of the collector size did not significantly affect the trajectories. For instance, the ion collection efficiency changes for only 2 % (which is well in the frame of the simulation uncertainty) when the size of the cubic grid is increased from 0.05 to 0.1 mm. In that respect, the most critical electrode for the calculation of the IG sensitivity is the grid: when the resolution is changed to 0.1 mm, the mean electron trajectory length is shorter for 37 % due to the reduced grid transparency.

## 4. Results and discussion

### 4.1 Estimative approach

The calculated distribution of electron trajectory lengths is presented in Figure 3. The peaks, periodically appearing at every  $\sim 40$  mm, can be readily observed. They correspond to electrons which pass 1, 2, 3... times over the ionisation region (i.e. the volume inside the grid) before hitting the grid. The peak close to the zero length corresponds to electrons that never enter the ionisation region, since they hit grid right after the emission from the filament. The mean electron trajectory path length equals about 132 mm.

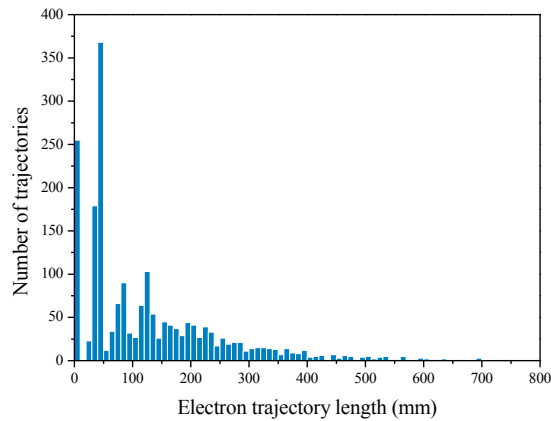


Figure 3. Distribution of electron path lengths inside the BA gauge.

The collection efficiency calculated from the simulations is 43.25 %. Interestingly, this magnitude is not uniform over the whole ionisation volume. Despite the long collector electrode, the collection efficiency is steady only in the proximity of the flange; at larger distances from the flange it decreases as can be seen in Figure 4. It should be noted that the change of the gas mass and/or temperature did not affect the collection efficiency.

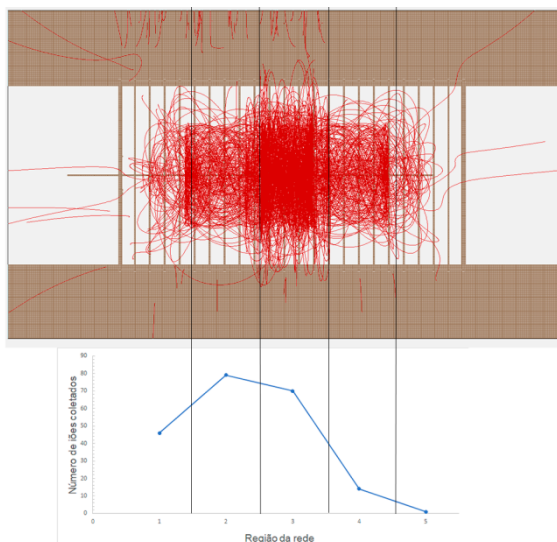


Figure 4. Illustration of ion trajectories inside the ionisation gauge, and the distribution of the ion collection efficiency along the gauge. Ricardo, tiff/jpg 300 dpi at least, and English. Increase the graph, vertical dimension, and then increase the font size

The remaining parameters necessary to estimate the gauge sensitivity are the gas temperature and the electron impact ionisation cross section. Since the current goal is to compare our result with the one obtained in [9], we choose the same gas temperature as the one chosen by the CERN group i.e. 300 K. The electron energy for which the cross section was calculated should be somewhat lower than 100 eV, the latter being the maximum electron energy inside the gauge. We arbitrary chose the electron energy of 85 eV. The ionisation cross sections for N<sub>2</sub> and H<sub>2</sub> were calculated using the BEB model, whilst that for Ar was taken from [17]. The parameters necessary to calculate the sensitivities for these three gases using the estimative approach  $S_{est}$  and the final results are presented in Table 3. The equivalent results obtained by the CERN group  $S_{CERN}$  [9] are also shown. The sensitivities obtained by the estimative approach agree very well with those of the CERN simulation in the case of H<sub>2</sub> and N<sub>2</sub>, while that for Ar is slightly below the lower margin of the simulation uncertainty. Probable reason for this slight discrepancy is in the cross section calculations. Indeed, the ionisation cross sections for the first two gases were obtained in the same way in both calculations, which is not the case for Ar.

Table 3. BA gauge sensitivities calculated using the estimative approach

Gas	$T$	$\langle L \rangle$	$P_{ion}$	$\sigma$ ( $10^{-20}$ m <sup>2</sup> )	$S_{est}$ (mbar <sup>-1</sup> )	$S_{CERN}$ (mbar <sup>-1</sup> )
H <sub>2</sub>	300 K	131.9 mm	0.4325	1.00	13.8	15.5 ± 2.3
N <sub>2</sub>				2.59	35.6	38.0 ± 5.7
Ar				2.70	37.2	45.1 ± 6.7

Very good agreement between the CERN simulations and the estimative approach reveals that small modifications of the electrodes' geometry due to the limited resolution and reduced volume of the chamber containing IG did not affect significantly the calculation of the sensitivity. Besides, neglecting space charges is apparently not of

major concern for this gauge since the agreement between the two results is not affected by the ion mass. However, CERN simulations show that the electron trajectories are shortened while the ion collection efficiency is increased due to the space charges. The two contributions practically compensate so that their net effect on the sensitivity is negligible [9].

The results presented in this section clearly show that estimative approach can provide quick and highly relevant result for the sensitivities. Some of the limitations of this approach were already discussed in Section 2.1. In addition, this approach is not suitable for further development that could include other physical phenomena such as space charging or electron backscattering from the grid. These drawbacks motivated us to work on a more complex approach that would allow simple upgrade for implementation of additional effects.

## 4.2 Monte Carlo simulation

The Monte Carlo simulation introduced in Section 2.2 allows evaluating the contribution of each electron trajectory to the ion current, including the consideration of the energy dependent ionisation cross section. Besides, the influence of electron backscattering from the grid on the gauge sensitivity is modelled, to our knowledge, for the first time. The snapshots of the trajectory calculations are depicted in Fig. 5a. The trajectories of primary electrons, backscattered electrons and ions are depicted by black, green and red lines, respectively. If we remove the figure 5a, which is also my suggestion, the previous two sentences will be omitted as well.

Since ion collection efficiency in our simulations does not depend on the initial ion velocity (i.e. on the gas temperature and the ion mass), ionisation cross section is the only gas dependent parameter which affects the gauge sensitivity. In other words,

differences between the simulations performed with different gases can be attributed exclusively to the ionisation cross section. All simulations presented in this work were therefore performed for  $N_2$ , which represents sufficient test of the model.

Calculated gauge sensitivity vs. the pressure with and without the consideration of backscattered electrons (BSE) is shown in Fig. 5. The relative uncertainty of the sensitivity obtained as the standard deviation of  $S$  for the 20 repeated simulations is  $\pm 5.5\%$  and  $\pm 3.4\%$  with and without including BSEs, respectively. It can be seen that the difference between the sensitivities for different pressures is in the frame of this uncertainty, as expected and experimentally confirmed for BA ionisation gauges [2]. The only exception from this general trend is sensitivity for  $1 \cdot 10^{-3}$  mbar, which is below the uncertainty margin in both cases (i.e. with and without BSE). The relative drops in sensitivity for the highest pressures are  $15.3\%$  (without BSE) i.e.  $12.2\%$  (without BSE). This sensitivity drop at higher pressures will be discussed below.

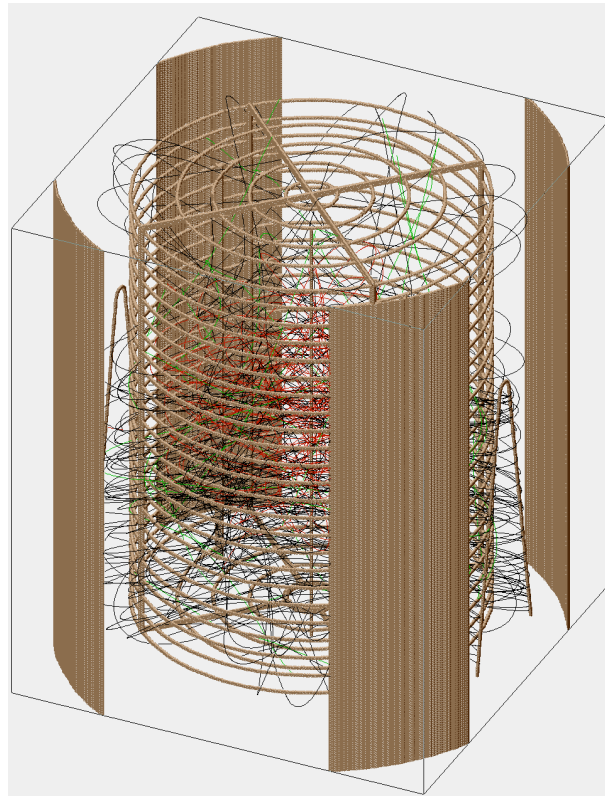


Figure 5a. Snapshot of the trajectory simulation using Simion. The trajectories of primary electrons, backscattered electrons and ions are presented as black, green and red lines, respectively. Ricardo, tiff/jpg 300 dpi at least

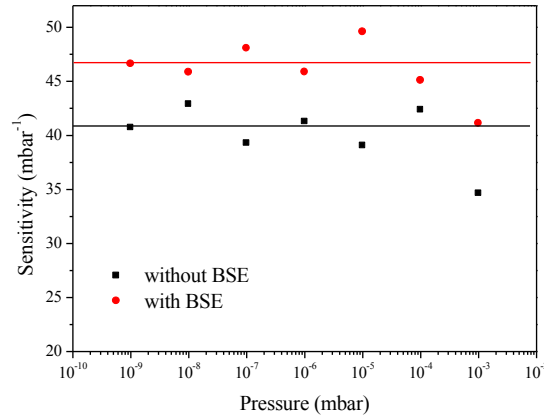


Figure 5. BA gauge sensitivity vs. nitrogen pressure calculated with and without considering BSEs. The average sensitivities in the pressure range  $10^{-9} - 10^{-4}$  mbar are denoted by the corresponding lines.

The mean value of the gauge sensitivity without BSEs is  $40.9 \pm 1.4 \text{ mbar}^{-1}$ . The result is slightly above the corresponding  $S_{\text{CERN}}$  value, well inside the uncertainty margins (cf. Table 3). It appears that the estimative approach somewhat underestimates the sensitivity, which can be explained by the arbitrary choice of the electron energy for which the ionisation cross section was calculated. Indeed, the average energy along the typical trajectory paths is around 80 eV, for which the cross section is indeed higher.

Ricardo, do we have a confirmation for this?

The gauge sensitivity increases to  $46.8 \pm 2.6 \text{ mbar}^{-1}$  when the contribution of BSEs is included. Their relative contribution was discussed qualitatively in [18], where its magnitude was suggested to be  $\sim 10\%$ . The contribution of BSEs to the gauge sensitivity evaluated from this simulation is about 14.4%. It should be noted that the

reliability of this result depends on the accuracy of the energy and incident angle dependent velocity distribution of BSEs. Since such comprehensive measurements were not found in the literature, the most feasible way of gaining this information would be via detailed Monte Carlo simulations of electron-material interactions.

The physical model implemented in the Monte Carlo simulation is correct as long as the calculated number of electrons in the bunch represented by a single trajectory is greater than 1. If this condition is not fulfilled, the probability that one electron can make more than a single ion cannot be neglected anymore. Therefore, transformation of the single electron into an ion will underestimate the sensitivity factor. In order to check if the observed small drop of  $S$  is due to failure of the physical model, we present in Fig. 6 part of the distribution of the number of electrons per trajectory  $f(N < 120)$  in the simulations for  $10^{-3}$  and  $10^{-4}$  mbar of nitrogen. The distributions, obtained by calculating 422 random trajectories, reveal that the relative amount of trajectories with  $N = 1$  is around 34 % for  $10^{-3}$  mbar, whilst this event was not registered for  $10^{-4}$  mbar. This confirms that the model fails for  $10^{-3}$  mbar of nitrogen, since the creation of more than a single ion per primary electron cannot be neglected. In addition, ionisation by secondary electrons, previously created in the process of ionisation, should be also considered under these circumstances. Encompassing these effects would be possible only by detailed modelling of the electron-molecule collisions, which is out of the scope of this approach. Finally, this result also implies that the approach proposed Kauert et al. [8], in which simulations were performed for pressures in the range  $10^{-3} - 10$  mbar, most probably underestimates the sensitivity.

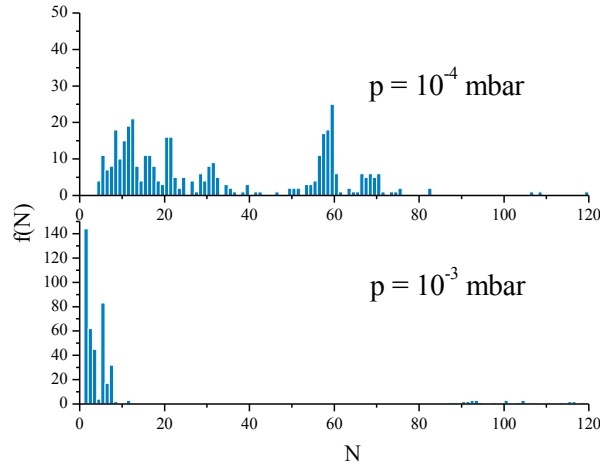


Figure 6. Distribution of the number of electrons per trajectory  $f(N)$  in the case of nitrogen at  $10^{-3}$  and  $10^{-4}$  mbar. Only the trajectories with the electron number less than 120 are considered.

## 5. Conclusion

Two approaches for the modelling of hot filament ionisation gauges using Simion program were introduced and compared with the recent equivalent work done in CERN [9]. All calculations can be readily executed on ordinary PC. The estimative approach, which can be simply implemented, is based on the calculation of electron path length and ion collection efficiency from the trajectory calculations. The more detailed one uses Monte Carlo method, apart from the calculation of electron/ion trajectories, to model the ionisation event.

While the estimative approach provides quantitatively highly relevant magnitude for the sensitivity, it omits to describe many important physical phenomena. The later can be readily achieved by the second approach, in which different effects (e.g. evaluating contribution of each electron trajectory, considering energy dependent ionisation probability etc.) can be implemented in a straight forward manner. In the present version of the code we model, for the first time, the gas ionisation by the

electrons backscattered from the grid. The first results show that they contribute to about 14 % of the overall gauge sensitivity.

## References

- [1] C. R. Tilford, Sensitivity of hot cathode ionization gauges, *J. Vac. Sci. Technol. A* 3 (1985) 546-550.
- [2] P.C. Arnold, S.C. Borichevsky, Nonstable behaviour of widely used ionization gauges, *J. Vac. Sci. Technol. A* 12 (1994) 568-573
- [3] D.G. Bills, Causes of nonstability and nonreproducibility in widely used Bayard-Alpert ionisation gauges, *J.Vac.Sci.Technol. A* 12 (1994) 574-579
- [4] T.J. Turner, C. Priestland, Sensitivity variations in the Bayard-Alpert ionisation gauge, Part II: Simulations of ion collection, for collimated beam input and chaotic gas input, using a digital computer, *Vacuum* 18 (1968) 319-326
- [5] S. Suginuma, M. Hirata, Dependence of sensitivity coefficient of a nude-type Bayard-Alpert gauge on the diameter of an envelope, *Vacuum* 53 (1999) 177-180
- [6] D.G. Bills, P.C. Arnold, S.L. Dodgen, C.B. Van Cleve, New ionization gauge geometries providing stable and reproducible sensitivities, *J.Vac.Sci.Technol. A* 2 (1984) 163-167
- [7] P.C. Arnold, D.G. Bills, M.D. Borenstein, S.C. Borichevsky, Stable and reproducible Bayard-Alpert ionization gauge, *J.Vac.Sci.Technol. A* 12 (1994) 580-586
- [8] R. Kauert, O.F.O. Kieler, St. Biehl, W. Knapp, Chr. Edelmann and St. Wilfert, Numerical investigations of hot cathode ionisation gauges, *Vacuum* 51 (1998) 53-59
- [9] P. Juda, B. Jenninger, P. Chiggiato, T. Richard, 3D-simulation of ionisation gauges and comparison with measurements, *Vacuum* 138 (2017) 173-177

- [10] P.J. Abbott, J.P. Looney, P. Mohan, The effect of ambient temperature on the sensitivity of hot-cathode ionization gauges, *Vacuum* 77 (2005) 217-222
- [11] W. Hwang, Y.-K. Kim, M.E. Rudd, New model for electron-impact ionization cross sections of molecules, *J. Chem. Phys.* 104 (1996) 2956-2966
- [12] M.A. Lennon, K.L. Bell, H.B. Gilbody, J.G. Hughes, A.E. Kingston, M.J. Murray, F.J. Smith, Recommended data on the electron impact ionisation of atoms and ions: fluorine to nickel, *J. Phys. Chem. Ref. Data* 17 (1988) 1285-1363
- [13] H. Seiler, Secondary electron emission in the scanning electron microscope, *J. Appl. Phys.* 54 (1983) R1-R18
- [14] D. Drouin, A.R. Couture, D. Joly, X. Tastet, V. Aimez, R. Gauvin, CASINO V2.42—A fast and easy-to-use modeling tool for scanning electron microscopy and microanalysis users, *Scanning* 9 (2007) 92-101.
- [15] M. M. El Gomati, C.G.H. Walker, A.M.D. Assa'd, M. Zadražil, Theory experiment comparison of the electron backscattering factor, from solids at low electron energy (250–5,000 eV), *Scanning* 30 (2008) 2-15
- [16] J. Wagner, J. Stummer, M. Völkerer, A. Hanke, J. Wernisch, Measuring the angular dependent energy distribution of backscattered electrons at variable geometry, *Scanning* 27 (2005) 298-304
- [17] H.C. Straub, P. Renault, B.G. Lindsay, K.A. Smith, R.F. Stebbings, Absolute partial and total cross sections for electron-impact ionization of argon from threshold to 1000 eV, *Phys. Rev. A* 52 (1995) 1115-1124
- [18] Grosse G., Harten U., Jitschin W., Gentsch H., Secondary electrons in ion gauges, *J Vac Sci Technol A* 1987;5(5):3242-43